Advances in Atmospheric Sciences
Impact Factor: 3.158
E-alert
ISSN 0256-1530
CN 11-1925/O4

An Interdecadal Change in the Influence of the NAO on Atlantic–Induced Arctic Daily Warming around the Mid–1980s

Cen WANG, Baohua REN, Gen LI, Jianqiu ZHENG, Linwei JIANG, Di XU

Citation: Wang, C., B. H. Ren, G. Li, J. Q. Zheng, L. W. Jiang, and D. Xu 2023: An Interdecadal Change in the Influence of the NAO on Atlantic–Induced Arctic Daily Warming around the Mid–1980s, *Adv. Atmos. Sci.*, 40, 1285–1297. doi: 10.1007/s00376–022–2218–8.

View online: https://doi.org/10.1007/s00376–022–2218–8

ADVANCES IN ATMOSPHERIC SCIENCES, VOL. 40, JULY 2023, 1285–1297

• **Original Paper** •

An Interdecadal Change in the Influence of the NAO on Atlantic-Induced Arctic Daily Warming around the Mid-1980s

Cen WANG[1], Baohua REN[*1], Gen LI[2], Jianqiu ZHENG[*1], Linwei JIANG[1], and Di XU[1]

[1]*School of Earth and Space Sciences*, *University of Science and Technology of China*, *Hefei* 230026, *China*
[2]*College of Oceanography*, *Hohai University*, *Nanjing* 210098, *China*

(Received 31 July 2022; revised 5 November 2022; accepted 28 November 2022)

ABSTRACT

After approaching 0°C owing to an Atlantic storm at the end of 2015, the Arctic temperature approached freezing again in 2022, indicating that Arctic daily warming events remain a concern. The NCEP/NCAR Reanalysis dataset was used to investigate the influence of the NAO on the Arctic winter daily warming events induced by Atlantic storms, known as the Atlantic pattern-Arctic Rapid Tropospheric Daily Warming (Atlantic-RTDW) event. Atlantic-RTDW events are triggered by Atlantic storms that transport warm and humid air masses moving into the Arctic. Furthermore, an interdecadal change in the influence of NAO on Atlantic-RTDW-event frequency was observed around the mid-1980s. Specifically, before the mid-1980s (pre-transition period), 500-hPa southerly (northerly) wind anomalies occupied the North Atlantic (NA) in the positive (negative) phase of NAO, which increased (decreased) the Atlantic-RTDW events occurrence by steering Atlantic storms into (away from) the Arctic; thus, the NAO could potentially influence the Atlantic-RTDW-event frequency. However, the relationship between the NAO and the Atlantic-RTDW-event frequency has weakened since the mid-1980s (post-transition period). In the post-transition period, such 500-hPa southerly (northerly) wind anomalies over the NA hardly existed in the positive (negative) phase of NAO, which was attributed to a stronger Atlantic Storm Track (AST) activity intensity than that in the pre-transition period. During this period, the strong AST induced an enhanced NAO-related cyclone via transient eddy-mean flow interactions, resulting in the disappearance of southerly and northerly wind anomalies over the NA.

Key words: Arctic daily warming, NAO, interdecadal change, Atlantic storm track, transient eddy-mean flow interactions

Citation: Wang, C., B. H. Ren, G. Li, J. Q. Zheng, L. W. Jiang, and D. Xu, 2023: An interdecadal change in the influence of the NAO on Atlantic-induced Arctic daily warming around the mid-1980s. *Adv. Atmos. Sci.*, **40**(7), 1285−1297, https://doi.org/10.1007/s00376-022-2218-8.

Article Highlights:

- Atlantic-induced Arctic daily warming events are triggered by Atlantic storms with warm and humid air masses.
- The influence of the NAO on Atlantic-RTDW events frequency underwent an interdecadal change around the mid-1980s.
- The interdecadal change is attributed to a strengthened Atlantic storm track activity intensity.

1. Introduction

An extreme Arctic daily warming event in the mid-winter of 2015 drew widespread attention from academia and the media when the North Pole surface air temperature rose by nearly 30°C in 24 h to warm above the freezing point (Boisvert et al., 2016; Moore, 2016). This event was a synoptic-scale process, as opposed to the well-recognized Arctic amplification, wherein the rising rate of Arctic mean temperature in winter is twice that of the rest of the Northern Hemisphere (NH; e.g., Graversen et al., 2008; Screen and Simmonds, 2010). Several studies have revealed that an intense Atlantic windstorm named Frank transported a huge, warm, and humid air mass into the Arctic hinterland, thus serving as the essential trigger for this extreme Arctic daily warming event. (Boisvert et al., 2016; Moore, 2016; Kim et al., 2017). Although the storm was short-lived, the warming was sustained for a long time owing to continuous blocking (Overland and Wang, 2016; Kim et al., 2017). Boisvert et al. (2016) found that a daily warming event melted 10 cm of ice in the Barents-Kara Sea region. Additionally, a cold air mass poured into the densely populated NH area following the daily warming event (Wang et al., 2019). These results demonstrate that an extreme Arctic daily warming event in winter could trigger a chain of atmospheric and marine inter-

* Corresponding authors: Baohua REN, Jianqiu ZHENG
Emails: ren@ustc.edu.cn, qiu@ustc.edu.cn

actions that are not limited to the local environment, potentially affecting populated areas.

It is noteworthy that, according to historical temperature records, this extreme Arctic winter daily warming event is not the only one, and such events have occurred occasionally in recent decades. Graham et al. (2017) found that Arctic temperatures in winter above –5°C were observed approximately three times per decade, and temperatures above –10°C occurred much more frequently. Furthermore, the frequency of daily warming events is increasing (Moore, 2016; Graham et al., 2017). Given that such warming events occur every winter and have significant societal impacts, we intend to determine what climatic conditions could determine and predict the frequency of Arctic winter daily warming events.

Several studies have identified that warming events are determined by Atlantic storm systems that transport heat and water vapor across the North Pole (e.g., Overland and Wang, 2016; Graham et al., 2017; Kim et al., 2017; Wang et al., 2019). Furthermore, the 500-hPa mean flow determines the cyclone track to a certain extent (Murray and Simmonds, 1995; Zhu et al., 2000; Hoskins and Hodges, 2002; Pinto et al., 2005). Thus, the 500-hPa mean flow has the potential to impact wintertime Arctic daily warming events.

The dominant low-frequency mode over the wintertime North Atlantic (NA) is termed the North Atlantic oscillation (NAO), which comprises simultaneous changes in the Icelandic Low (IL) and the Azores High (AH; Barnston and Livezey, 1987). Moreover, the IL, a wintertime semi-permanent surface low pressure (SLP) center over the NA northern basin, is not only a cyclogenesis region, but cyclone from the south usually converges here, especially in winter (e.g., Blackmon et al., 1984; Serreze et al., 1997). The IL and NAO closely establish the synoptic variability and mean flow (Lau, 1988; Hurrell, 1995a). Thus, these features may significantly impact the NA and elsewhere on diverse timescales (Hurrell, 1995a; Serreze et al., 1997; Thompson and Wallace, 2001). Several studies have verified that the cyclone tracks over the NA display a poleward orientation during the positive phase of the NAO (Rogers, 1990; Hurrell, 1995b). Therefore, we anticipate that the NAO will impact cyclone tracks related to Arctic daily warming events during winter.

Furthermore, the NAO demonstrates clear decadal variability (Woollings et al., 2015). Since the early 1950s, the NAO has experienced pronounced interdecadal changes (Hurrell, 1995a; Woollings et al., 2015). The Atlantic Storm Track (AST) significantly contributes to the IL and NAO maintenance and development via transient eddy forcing (Honda et al., 2001; Honda and Nakamura, 2001).

Our previous studies defined the Atlantic pattern-Arctic winter daily warming event (Atlantic-RTDW; Wang et al., 2019, Figs. 1 and 2; Section 3). In the current study, we attempt to link the Atlantic-RTDW-event frequency to the large-scale atmospheric circulation and focus on the relationship between the NAO and the Atlantic-RTDW-event frequency.

The remainder of this paper is organized as follows. In section 2, the data and methods are introduced. Section 3 describes the synoptic-scale processes of Atlantic-RTDW. Section 4 examines the change in the relationship between the Atlantic-RTDW-event frequency and the NAO. The physical processes underlying the change in the relationship between the NAO and the Atlantic-RTDW-event frequency are presented in section 5. Section 6 provides a conclusion for the study.

2. Data and methods

2.1. *Data*

We utilized reanalysis data from the National Centers for Environmental Prediction/National Center for Atmospheric Research (NCEP/NCAR) Reanalysis (Kalnay et al., 1996; available at the website: https://psl.noaa.gov/data/gridded/reanalysis/), including daily and monthly geopotential height and horizontal winds at standard pressure, and daily 1000-hPa temperatures at on 2.5° × 2.5° latitude-longitude grids from 1950 to 2019. We also utilized the ERA5 reanalysis from the European Center for Medium-Range Weather Forecasts (ECMWF; Hersbach et al., 2020), including those geophysical fields on 0.25° × 0.25° latitude-longitude grids from 1950 to 2019.

To define Arctic daily warming in this study, the daily temperature data were preprocessed as follows. First, the daily mean temperature was converted to the "daily temperature increment", defined as the difference between the temperature of the day of interest and the previous day's temperature. Then, to remove the seasonal cycle, we conducted an operation in which the average temperature increment for a given calendar day for the winters of 1950–2018 was subtracted from the actual temperature increment of that day. We called this result the "daily temperature increment anomaly". For example, the "daily temperature increment anomaly" on 1 December 2000 is the "daily temperature increment" averaged over every December 1 from 1950 to 2018 subtracted from the "daily temperature increment" on 1 December 2000. In this way, we obtained 6227 days of the "daily temperature increment anomaly" in the winters of 1950–2018.

The monthly NAO index for 1950–2019 was acquired from the NOAA Climate Prediction Center (CPC; available at the website: https://psl.noaa.gov/data/climateindices/list/). Rotated Principal Component Analysis (RPCA; Barnston and Livezey, 1987) was used for three-month mean 500-hPa height anomalies in the region 20°–90°N, and ten leading EOFs were selected. The time series of the first mode is the NAO index.

For significance testing of the regression and composite analyses, a two-tailed Student's *t*-test was used in our study.

2.2. *Storm track activity*

The storm track activity (also known as synoptic-scale

eddy activity) was defined in our study as the root mean square (RMS) of the 2–8-day bandpass filtered geopotential height at 300 hPa (Blackmon et al., 1977; Lee et al., 2012).

2.3. *Extended Eliassen–Palm flux*

The horizontal flux components of the extended EP flux, which can qualitatively characterize the dynamic interaction between the transient eddy and mean flow (Hoskins et al., 1983), as modified by Trenberth (1986), are written as:

$$\boldsymbol{E}_u = \left[\frac{1}{2}\left(\overline{v'^2} - \overline{u'^2}\right)\boldsymbol{i} - \overline{u'v'}\,\boldsymbol{j}\right]\cos\varphi\,, \tag{1}$$

where u' and v' are the zonal and meridional winds on a synoptic scale, respectively, and φ is latitude. The synoptic-scale horizontal winds were obtained using a Butterworth bandpass filter to retain the fluctuating components for 2–8 days (Murakami, 1979). The overbar represents the average taken over the winter-season timescale.

2.4. *Geopotential height tendency*

In addition to qualitatively diagnosing EP flux, we used the geopotential height tendency equation to quantitatively estimate the feedback of the transient eddies to the mean flow. The equivalent barotropic geopotential height tendency response to the transient eddy vorticity forcing can be diagnosed following Cai et al. (2007):

$$\frac{\partial h}{\partial t} = \nabla^{-2}\left[-\frac{f}{g}\nabla\cdot\left(\boldsymbol{v}_h'\xi'\right)\right], \tag{2}$$

where $\partial h/\partial t$ denotes the geopotential height tendency, and f and g are the Coriolis parameter and the gravitational acceleration, respectively. $\boldsymbol{v}_h'$ and ξ' are the synoptic-scale horizontal wind and relative vorticity, respectively, which are applied for 2–8-day filtering with a Butterworth bandpass filter (Murakami, 1979).

3. Definition and meteorological conditions of the Atlantic-RTDW event

3.1. *Definition of the Atlantic-RTDW event*

We define a rapid tropospheric daily warming (RTDW) event as any day during the situ winter (December–February) from 1950 to 2018 when the "daily temperature increment anomaly" at 1000 hPa averaged over the region north of 66.5°N is warmer than one standard deviation above the mean, where the standard deviation is based upon the 6227 "daily temperature increment anomalies" for the winters of 1950 to 2018. Successive RTDW days are counted separately. Compositing weather condition fields on the days of RTDW event occurrence could then be used to describe the RTDW event. There are two paths by which southerly wind anomalies can enter the Arctic, one from the Atlantic Ocean and the other from the Pacific Ocean, and the surface pressure fields corresponding to the different southerly wind anomalies are also quite different (figure omitted; Wang et al., 2019). Given that the Atlantic and Pacific Oceans are different sources of heat in the Arctic, we suspect that RTDW events could be classified into diverse types. The classification results are demonstrated below.

To improve classification accuracy, we used two different methods to classify RTDW events: the k-means (Mirkin, 1996) and fuzzy c-means method (FCM; Fujibe, 1989, 1999). We set the number of clusters to two, and other parameters were selected by default for classification methods. We then conducted a cluster analysis of the meridional wind anomalies for RTDW-event occurrence days. Both classification methods produce results that divide RTDW events into Atlantic- and Pacific-RTDW events, which intuitively correspond to RTDW events with southerly wind anomalies from the Atlantic and Pacific Oceans, respectively (Fig. 1; Wang et al., 2019). In all, 454 Atlantic- and 437 Pacific-RTDW events in winter were obtained for 1950–2018. Because the results of the two classification methods were consistent, we present the FCM classification results. Moreover, this study focuses on the Atlantic-RTDW event.

Figure 1 depicts the anomalous atmospheric conditions when Atlantic-RTDW events occur. An anomalous cyclone appears over Greenland, and an anticyclonic anomaly is located over northern Eurasia. Furthermore, under the combined actions of the cyclone and anticyclone, a strong southerly wind anomaly between these two systems enters the Arctic region from the Atlantic Ocean. Due to the heat energy from the Atlantic Ocean transported by the cyclone,

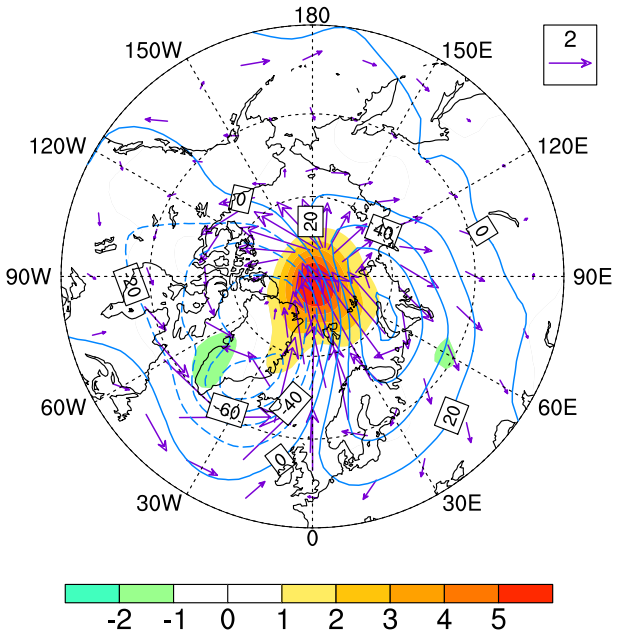

Fig. 1. Synoptic anomalous atmospheric conditions at 1000 hPa when Atlantic-RTDW events occur, including temperature increments (colored, contour interval: 1, units: °C), geopotential height (blue contours, contour intervals: 20, units: m), and horizontal wind (purple vector, units: m s^{-1}). The vector scale is depicted in the top right, the same as below. Figure 1 is a composite using all Atlantic-RTDW days.

the Arctic air temperature rose increased by 5°C in just one day. The Pacific Ocean is another energy source for the Arctic (Graham et al., 2017; Wang et al., 2019), as such, humid and warm air masses from the Pacific Ocean could also trigger Arctic daily warming. This is called a Pacific-RTDW event. The Pacific- and Atlantic-RTDW events are different but related, and their relationship deserves further study.

3.2. *Atmospheric conditions from the initial to the peak Atlantic-RTDW event date*

To offer a more thorough introduction to Atlantic-RTDW events, we described the conditions leading up to and during an event (Fig. 2). At the initial date of an Atlantic-RTDW event (three days before the occurrence of the Atlantic-RTDW events), a deep trough in the mid-troposphere was located over western Greenland, while a ridge was located over eastern Iceland. The position between the deep trough and ridge at the upper level favors cyclogenesis. Furthermore, the cyclone moves northward into the Arctic along southerly winds (e.g., Zhu et al., 2000; Pinto et al., 2005). At the surface, a depression center can be visualized between Iceland and Greenland on the initial date. It then moved northward over the next few days. On the peak Atlantic-RTDW event date, the storm arrived at the North Pole, with unusually strong southerly wind anomalies (maximum over 6.0 m s^{-1}) from the Atlantic Ocean crossing toward the North Pole along the prime meridian (0° longitude).

4. Definition of the Atlantic-RTDW index and its relationship with NAO

4.1. *Definition of the Atlantic-RTDW index*

From 1950 to 2018, we obtained 454 Atlantic-RTDW events in winter. These events occur 6.6 times, on average, during winter, with a maximum of 14 times and a minimum of 0. The number of Atlantic-RTDW event occurrences in a given winter (also called the Atlantic-RTDW-event frequency) is defined as the Atlantic-RTDW index. Therefore, this index can be used to explore the relationship between the climatic index (e.g., NAO) and the Atlantic-RTDW-event frequency (the time series of the Atlantic-RTDW index is depicted in Fig. 3).

As previously stated, a cyclone entering the Arctic is critical for Atlantic-RTDW event occurrence. Furthermore, Atlantic cyclones that are strongly related to the NAO phase have been demonstrated in numerous studies (e.g., Magnusdottir et al., 2004; Hanley and Caballero, 2012). Thus, our study focused on the relationship between the NAO and Atlantic-RTDW events. The cyclone track moves northward (southward) following the southerly (northerly) mean wind flow in the middle troposphere (e.g., Murray and Simmonds, 1995; Zhu et al., 2000). Therefore, if the positive (negative) phase of NAO offers favorable (unfavorable) conditions, such as southerly (northerly) wind mean flow in the middle troposphere for cyclones entering (away) the Arctic from

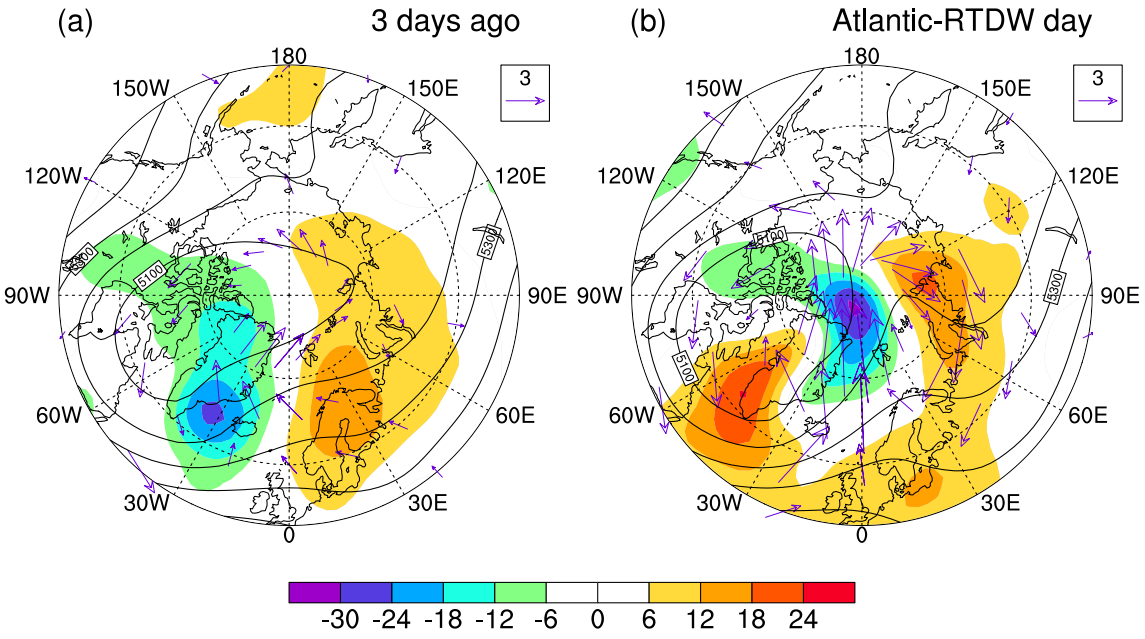

Fig. 2. Synoptic atmospheric conditions at (a) 3 and (b) 0 days before an Atlantic-RTDW event occurrence, including the geopotential height (black contours, interval: 100, units: m) and 500-hPa horizontal wind anomaly (purple vector, units: m s^{-1}) and 24-hour isallobar anomaly at 1000 hPa (colored, interval: 6, units: m). The arrows depict horizontal wind anomalies with meridional component anomalies that are significant at the 99% level. The "24-hour allobar" helps to define a "24-hour isallobar". The former indicates the difference in the geopotential height between the day of interest and the prior day, while the latter represents a line running through places experiencing equal "24-hour allobars".

the Atlantic Ocean during winter, there will be more (less) Atlantic-RTDW events in winter. Simply put, the NAO and Atlantic-RTDW-event frequency have a positive relationship. If the positive (negative) phase of NAO cannot offer favorable (unfavorable) conditions, the relationship between the NAO and Atlantic-RTDW-event frequency would be weak. The specific relationship between the frequency of Atlantic-RTDW events and the wintertime NAO will be explored in the next subsection.

4.2. *The relationship change in the Atlantic-RTDW events frequency and NAO*

The Atlantic-RTDW-event frequency (measured by the Atlantic-RTDW index) is only weakly correlated with the wintertime NAO index (r=0.12; insignificant). At first glance, this finding indicates a lack of a connection between the Atlantic-RTDW-event frequency and the NAO. However, when one considers that the NAO phase has undergone a decadal-scale transition from a negative to an unprecedented positive phase, and that it has been mostly positive since the 1980s (Hurrell, 1995a; Woollings et al., 2015), we must acknowledge the possibility that the relationship between the NAO and Atlantic-RTDW index (representing the Atlantic-RTDW event-frequency) may have experienced an interdecadal change.

Figure 3 indicates that these two indices were mostly in phase prior to the mid-1980s but were less coherent after the mid-1980s. The 21-year moving correlation coefficients of the Atlantic-RTDW and NAO indices further demonstrate an interdecadal change around the mid-1980s. Specifically, Fig. 3 demonstrates that from 1981 to 1982 (from 1962 to 1963), the 21-year sliding correlation coefficient becomes statistically insignificant (significant) from significant (insignificant). The 21-year sliding correlation coefficient in 1981 (1963) represents the correlation coefficient between the Atlantic-RTDW and NAO from 1971–91 (1953–73). Thus, the 21-year sliding correlation coefficient was positive and statistically significant at the 95% level during 1963–81, representing the central years of 1953–91 (pre-transition period), but weakened during 1989–2002, representing the central years of 1979–2012 (post-transition period). We may define the pre-transition period as 1953–91 and the post-transition period as 1979–2012. Thus, 1979–91 is an overlapping period, divided equally into pre- and post-transition periods. As a result, we obtained two periods, one from 1953 to 1984 (pre-transition period) and the other from 1985 to 2012 (post-transition period).

This interdecadal change was reverified by the Atlantic-RTDW and NAO index scatter plots during 1953–84 and 1985–2012 (Fig. 4). The correlation coefficient between the Atlantic-RTDW and NAO indices was 0.53, statistically significant at the 99% level in the pre-transition period, but it had weakened and become insignificant in the post-transition period (–0.26). The results of the sliding correlation and scatterplots strongly suggest that the influence of the NAO on the Atlantic-RTDW-event frequency changed around the mid-1980s. This change requires further investigation.

5. Possible mechanisms for the change in the influences of the NAO on the Atlantic-RTDW-event frequency

5.1. *The Atlantic-RTDW pattern in two periods*

Before delving into the possible mechanisms, we must first identify the Atlantic-RTDW-related large-scale atmospheric circulation anomalies, known as the Atlantic-RTDW pattern, which represents the background conditions for Atlantic-RTDW event occurrence. If the NAO is consistent with the Atlantic-RTDW pattern, it could influence the Atlantic-RTDW-event frequency and vice versa.

Figure 5 demonstrates the regressions of winter geopotential height and horizontal wind speed anomalies in the mid-

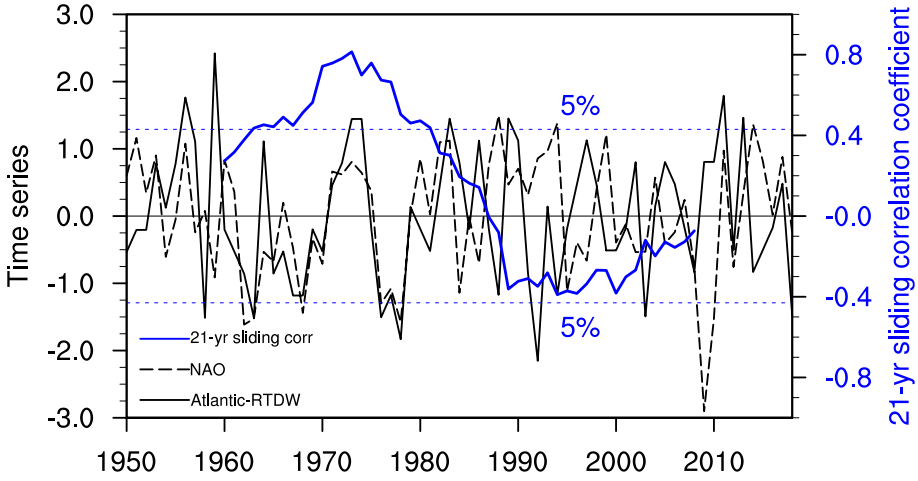

Fig. 3. The standardized Atlantic-RTDW index (solid black line) and winter NAO index (dotted black line) from 1950 to 2018. The solid blue line represents their 21-year sliding correlation coefficient (abbreviated "21-yr sliding corr"), and the dashed blue lines represent significance at the 95% level.

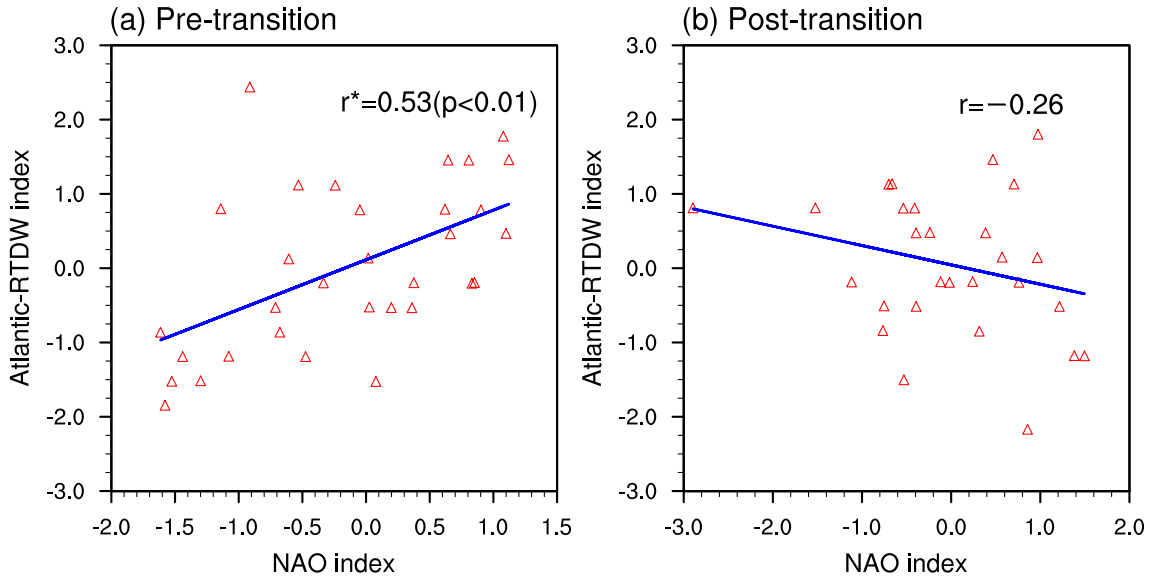

Fig. 4. Scatter plots of the standardized NAO and the Atlantic-RTDW indices during the (a) 1953–84 (pre-transition period) and (b) 1985–2012 (post-transition period), respectively. The *r*, *p*, and blue lines represent the correlation coefficient, *p*-value, and linear fit between these two indices, respectively.

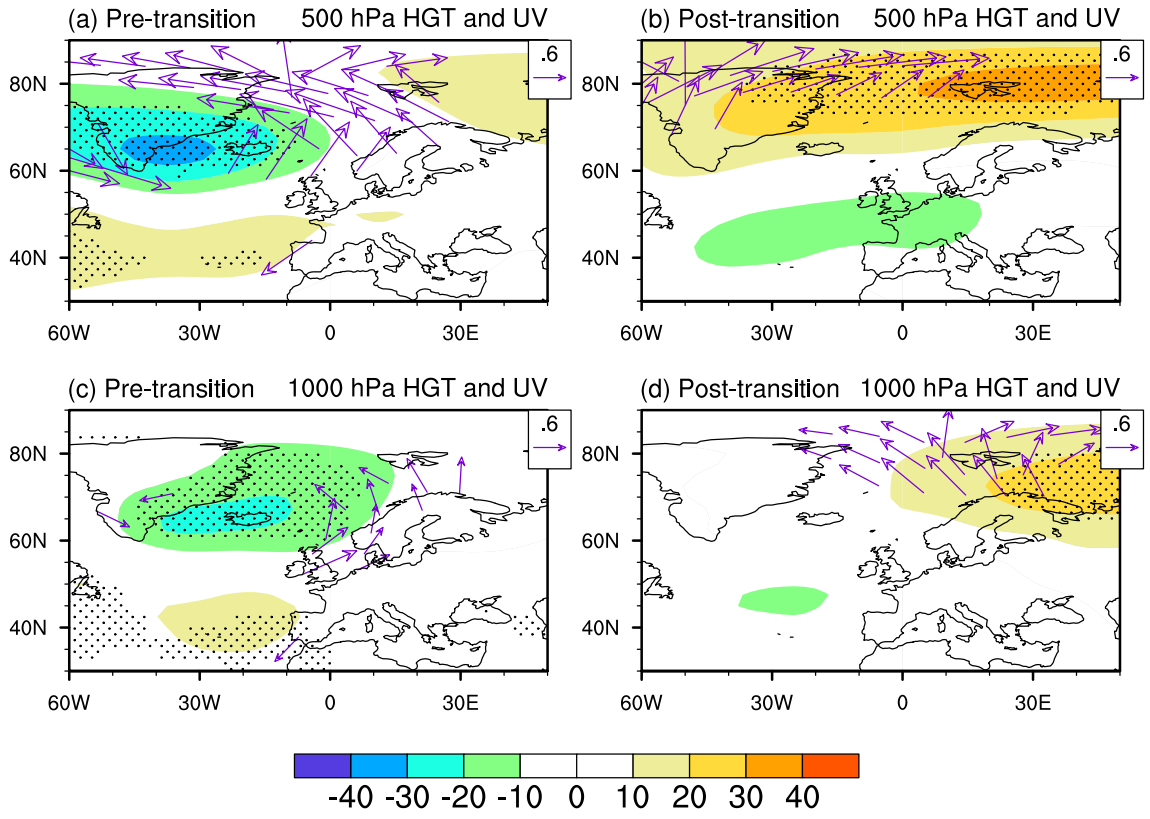

Fig. 5. Regressions of the geopotential height (colored, interval: 10, units: m) and horizontal wind speed (purple vector, units: m s^{-1}) anomalies at (a–b) 500 hPa and (c–d) 1000 hPa on the Atlantic-RTDW index during 1953–84 (pre-transition period; a, c) and 1985–2012 (post-transition period; b, d), respectively. The arrows depict the horizontal wind with meridional component anomalies significant at the 95% level. The dots denote significance at the 95% level for the geopotential height.

low troposphere on the Atlantic-RTDW index during the pre- and post-transition periods. During the pre-transition period, anomalous cyclonic and anticyclonic circulations appeared at 500 and 1000 hPa over Iceland and the Azores, respectively. The NAO pattern resembles the Atlantic-RTDW pattern during the pre-transition period, implying

that NAO is associated with the Atlantic-RTDW-event frequency. Conversely, there was only an anticyclonic anomaly over and to the north of the Barents and the Kara Seas during the post-transition period, implying a weak relationship between the NAO and the Atlantic-RTDW-event frequency. Although the Atlantic-RTDW patterns during the pre- and post-transition periods differed, the southerly wind anomalies were always along the prime meridian and occupied the North Atlantic (NA) during the two periods.

These results are consistent with those of section 3 and several previous studies, which demonstrate that southerly wind anomalies favor the Atlantic-RTDW-event frequency by causing the cyclone to move northward into polar regions (e.g., Murray and Simmonds, 1995; Zhu et al., 2000). It is hypothesized that the NAO could be associated with the Atlantic-RTDW-event frequency in the pre-transition period, which is attributed to the southerly (northerly) wind anomalies along the prime meridian in the positive (negative) NAO phase. However, if there are no southerly (northerly) wind anomalies in the positive (negative) NAO phase, the NAO cannot be related to the Atlantic-RTDW-event frequency. This assumption has now been verified. This study focuses on the change in the relationship between the Atlantic-RTDW-event frequency and NAO and the potential physical mechanisms for this change. The Atlantic-RTDW pattern in the post-transition period may resemble an Arctic Oscillation (AO)-like pattern (Thompson and Wallace, 1998). The factors influencing the Atlantic-RTDW pattern during the post-transition period may be complex and will be investigated in the future.

5.2. *The interdecadal changes in the NAO*

Several previous studies have demonstrated that the NAO phase experienced an interdecadal change in the 1980s and has since been positive in most years (Hurrell, 1995a; Luo et al., 2011; Woollings et al., 2015). Herein, we investigated whether the changes in the relationship between the NAO and the Atlantic-RTDW-event frequency are related to the phase change in the NAO index.

Figure 6 displays the 21-year sliding average of the NAO index (the NAO index phase change) and the 21-year sliding correlation coefficient between the Atlantic-RTDW index and NAO index (the change in the relationship between the NAO and Atlantic-RTDW indices). The 21-year sliding average of the NAO transitioned from a negative to a positive regime around the 1980s, implying an intensified Iceland Low and Azores High since the 1980s (Fig. 7). The average values of the NAO in 1953–84 and 1985–2012 are –0.49 and 0.3, respectively. Furthermore, by choosing 1984/1985 as a break period, a significant decadal regime shift of the NAO is evident according to the Student's t-test. Particular attention is given to the correlation coefficient of –0.42 (p<0.01) between the 21-year moving averages and correlations. The moderate correlation coefficient indicates a close linkage between the interdecadal change in the relationship between the two indices and the NAO phases. How do the different NAO phases during the pre-and post-transition periods result in distinct impacts on the Atlantic-RTDW event? To reveal the related mechanisms, we compared the NAO-related circulations during the positive NAO years between the two periods. Positive or negative NAO years in the pre-transition and post-transition periods with the NAO index exceeding ±1 standard deviation were identified.

Figure 7 depicts the geopotential height and horizontal 500-hPa wind speed composite anomalies for the two periods in the positive NAO years. During both periods, anomalous cyclones and anticyclones were located over Iceland and the Azores. However, the anomalous cyclone and anticyclone

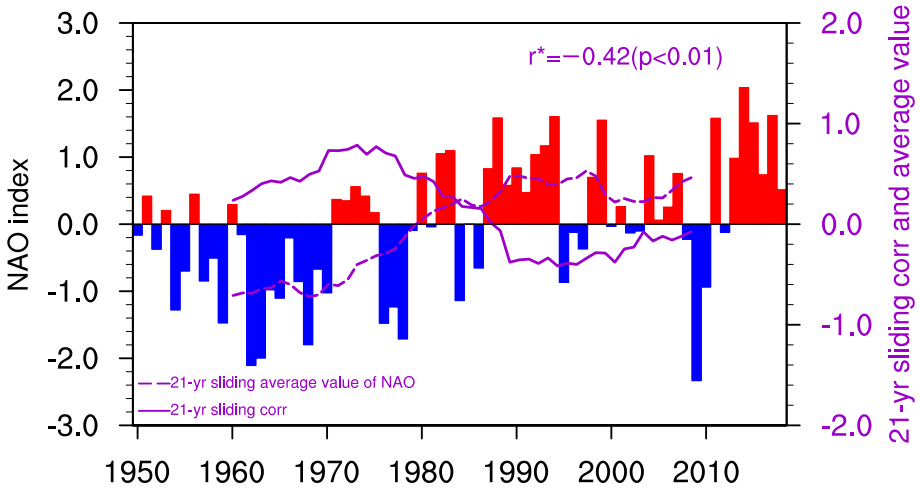

Fig. 6. The standardized NAO index (color bar, positive in red and negative in blue) from 1950 to 2018. The solid purple line represents the 21-year sliding correlation coefficient between the Atlantic-RTDW index and NAO index (abbreviated "21-yr sliding corr"), and the dashed purple line represents the 21-year sliding average value of the NAO index (abbreviated "21-yr sliding average value of the NAO"). The correlation coefficient is given by r, and the p-value indicates significance at the 99% level.

intensities were strengthened, corresponding to the increase in the NAO index from the pre- to post-transition period. As a result, in the pre-transition period, significant southerly wind anomalies to the east of the anomalous Iceland low occupy the NA, which is consistent with the Atlantic-RTDW pattern (Fig. 7a). Therefore, the NAO could be associated with the Atlantic-RTDW-event frequency during the pre-transition period. However, owing to the enhanced Iceland low anomaly, the significant southerly wind anomalies over the NA disappeared in the post-transition period, implying that the NAO could not establish a connection with the Atlantic-RTDW-event frequency during this period (Fig. 7b).

5.3. *Possible reasons for the interdecadal changes in NAO*

Significant discrepancies in the atmospheric circulation anomalies associated with the wintertime NAO between the pre- and post-transition periods have been described. Moreover, these significant differences determine the different relationships between the NAO and the Atlantic-RTDW-event frequency in the two periods. However, the cause of the significant discrepancies in NAO-related circulation anomalies over NA between the two periods remains obscure.

In Fig. 7, a more intense Azores High and deeper Iceland Low in the post-transition period resulted in a stronger meridional geopotential height gradient over the NA than in the pre-transition period, which suggests a stronger westerly jet stream. Figure 8 further demonstrates that in positive NAO years, the NAO-related westerly jet stream along 40°–60°N over the NA was stronger in the post-transition than in the pre-transition period. Furthermore, a stronger low-frequency mean flow is closely related to stronger storm track activity (also termed synoptic-scale eddy activity; Limpasuvan and Hartmann, 1999, 2000).

Previous studies have demonstrated that the feedback of synoptic-scale eddy activity to mean flow can sustain the main climate modes (e.g., Lorenz and Hartmann, 2001, 2003; Jin et al., 2006a, b). For example, the Atlantic storm track (AST) feedback onto the NAO via eddy-mean flow interactions has been verified in previous research (e.g., Orlanski, 1998; Kug and Jin, 2009). Specifically, a strengthened AST intensity helps to reinforce and maintain low-frequency tropospheric circulation changes by inducing a cyclonic tendency to its north and an anticyclonic tendency to its south (Lau, 1988; Lee et al., 2012). As a result, AST intensity changes may cause differences in the NAO-related circulation anomalies between the pre- and post-transition periods via

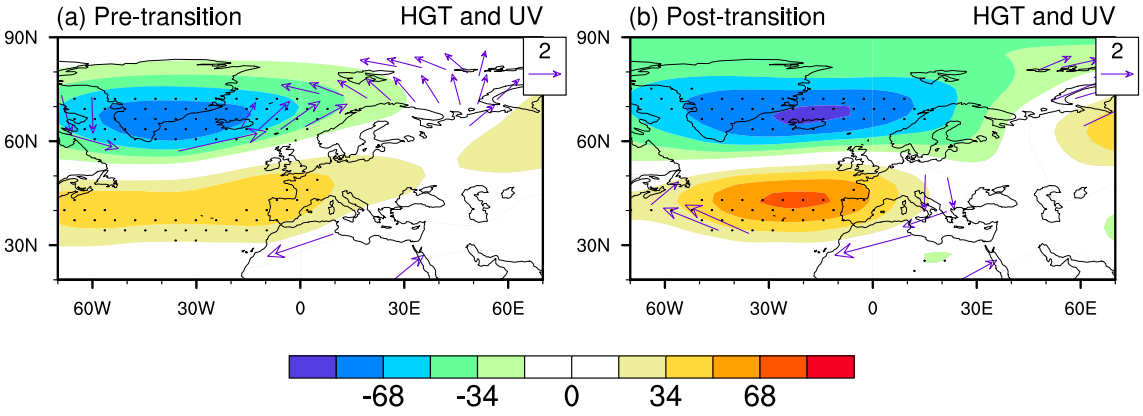

Fig. 7. Composites of geopotential height anomalies (colored, interval: 17, units: m) and horizontal wind speed anomalies (purple vector, units: m s^{-1}) at 500 hPa during the positive NAO years of 1953–84 (pre-transition period; a) and 1985–2012 (post-transition period; b), respectively. The arrows depict the horizontal wind with meridional component anomalies significant at the 95% level. The dots denote geopotential heights significant at the 95% level.

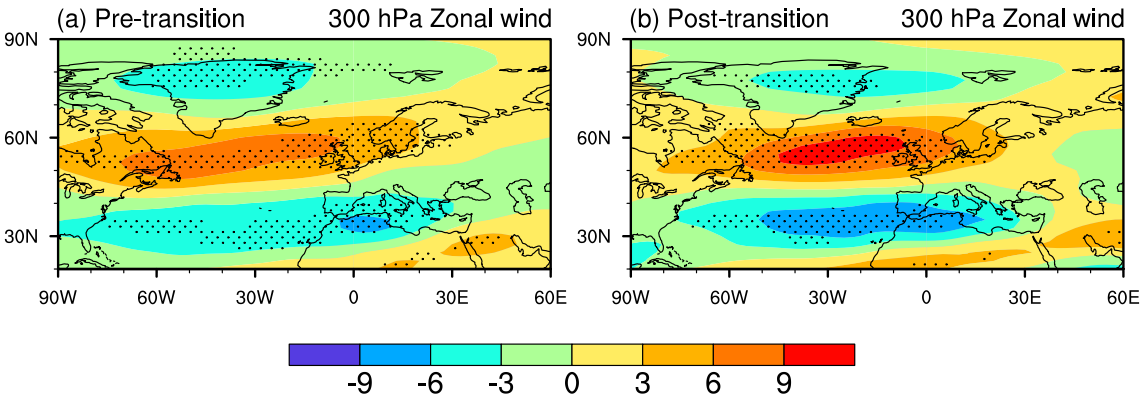

Fig. 8. As in Fig. 7, but for zonal wind speed anomalies at 300 hPa (colored, interval: 3, units: m s^{-1}).

eddy feedback to the mean flow. The changes in the AST during the two periods will then be presented.

Figure 9a depicts the post-transition period, wintertime AST activity and the differences between the post- and pre-transition periods. The post-transition period AST activity was much stronger at approximately 45°–60°N over the NA than in the pre-transition period, indicating that winter AST activity underwent a dramatic interdecadal change. The AST activity intensity index was calculated by averaging the standardized AST activity over 45°–60°N and 50°W–30°E (Fig. 9). Figure 9b further demonstrates a clear transition in AST activity intensity in the 1980s, from a weak regime in the former period to a strong regime in the latter. Several previous studies have verified the remarkable intensification of wintertime AST activities since the 1970s (Chang and Fu, 2002; Harnik and Chang, 2003; Lee et al., 2012). Furthermore, previous studies have demonstrated that the synoptic-scale eddy feedback strength to the low-frequency mean flow is directly proportional to storm track activity intensity (Jin et al., 2006a, b; Jin, 2010). Herein, the qualitative and quantitative dynamic diagnosis of the transient eddy feedback to the mean flow will be presented during the two periods.

The extended EP flux can qualitatively characterize the barotropic process in low-frequency atmospheric circulation anomalies forced by transient eddies (e.g., Hoskins et al., 1983; Lau, 1988). Specifically, EP flux divergence was accompanied by positive geopotential height tendencies to the south and negative geopotential height tendencies to the north and vice versa. Figures 10a and 10b depict the anomalies of the extended EP flux and their divergence associated with the standardized ATS activity intensity index during the pre-transition and subsequent periods. In both periods, the EP flux divergence dominated from 70°W to 30°E and 45° to 60°N, with positive eddy-induced geopotential height tendencies to its south and negative geopotential height tendencies to its north in the positive phase of the AST activity intensity index (Fig. 10). Furthermore, there were noticeable differences in the EP flux divergence and eddy-induced geopotential height tendencies during diverse periods. The differences in geopotential height tendency anomalies induced by eddy vorticity between the two periods (Figs. 10c–d) may support the different circulation anomalies associated with the NAO described above (Fig. 7). The EP flux divergence and eddy-induced geopotential height tendency anomalies were much stronger in the post-transition period than in the pre-transition period (Fig. 10). Strong negative and positive geopotential height tendencies strengthen the IL and AH, respectively, resulting in the disappearance of significant southerly wind anomalies over NA in the post-transition period. Therefore, the barotropic diagnostic suggests that changes in the transient eddy feedback to the mean flow associated with vorticity transportation may elucidate the NAO pattern changes over two periods, resulting in the interdecadal change in the influence of NAO on the Atlantic-RTDW-event frequency.

6. Summary and discussion

It is well known that Arctic warming strains not only local sea ice and ecosystems but also causes severe cold air outbreaks in densely populated low-to-mid-latitude regions, threatening lives and causing economic damage. Our work focuses on the Atlantic-RTDW event (Atlantic-induced Arctic winter daily warming event) and the relationship between the frequency of these events and the NAO.

Concerning the Atlantic-RTDW event, we found that the southerly/northerly anomalies within the mean flow over the NA are conditions for its occurrence. Previous research has discovered that the mean flow determines the storm movements. (e.g., Murray and Simmonds, 1995; Zhu et al., 2000). Consequently, a storm with a large warm and humid air mass could move into (away from) the Arctic by following the anomalous southerly (northerly) wind from the NA, causing (preventing) the occurrence of an Atlantic-RTDW event.

The relationship between the Atlantic-RTDW-event frequency and the NAO demonstrates an interdecadal change

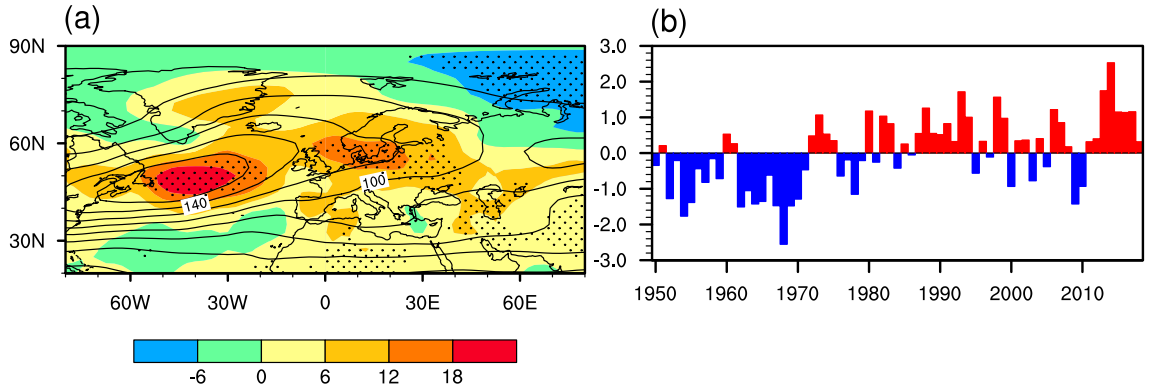

Fig. 9. (a) The wintertime AST activity during the post-transition period (contour, interval: 20, units: m); the difference in wintertime AST activity between the post- and pre-transition period (colored, interval: 6, units: m); the dots indicate that the anomalies differ from zero, significant at the 99% level. (b) The time series of the standardized winter AST activity intensity index, positive in red and negative in blue.

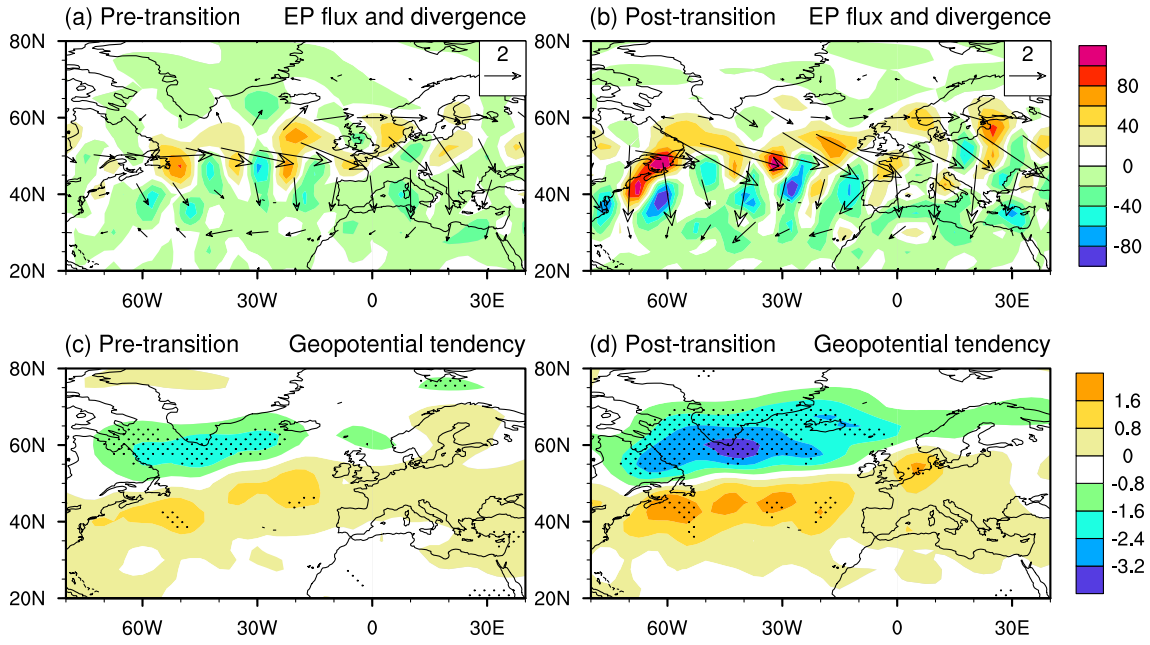

Fig. 10. Regressions of the extended EP flux anomalies (a, b; vector, units: $m^2\ s^{-2}$), divergence anomalies of the EP flux (a, b; colored, interval: 20, units: $m\ s^{-2}$) and the eddy-induced geopotential height tendency (c, d; colored, interval: 0.8, units: $m\ d^{-1}$) anomalies at 300 hPa on the standardized AST activity intensity index during the pre- (a, c) and post-transition (b, d) periods. The dots denote significance at the 98% level. For convenience, the EP flux divergence has been multiplied by 10^7.

around the mid-1980s, characterized by a strong correlation in the pre-transition period (1953–84), and a dramatically weakened correlation in the post-transition period (1985–2012). To evaluate whether the results were sensitive to adjusting the respective time windows of the periods, we recalculated the correlation coefficient between the Atlantic-RTDW and NAO by choosing 1981/1982, 1982/1983, 1983/1984, 1984/1985, 1985/1986, 1986/1987, and 1987/1988 as break periods. After adjusting the respective time windows of the periods, the correlation coefficients were still significant (0.49 to 0.60) in the pre-transition period, while it was weakened (–0.27 to –0.14) in the post-transition period. These results suggest that the interdecadal change in the influence of NAO on the Atlantic-RTDW-event frequency truly exists and does not depend on the selected time window of the periods. Moreover, using the ERA5 dataset, we recalculated the correlation coefficient between the Atlantic-RTDW and NAO indices in the pre-transition period (0.36; significant) and post-transition period (–0.27; insignificant), respectively [Fig. S1 in the electronic supplementary material (ESM)]. The results obtained using the ERA5 dataset verify that this interdecadal change in the NAO's influence on the Atlantic-RTDW-event frequency around the mid-1980s is robust.

In the pre-transition period, the NAO pattern resembles the Atlantic-RTDW pattern, and the southerly and northerly wind anomalies occupy the NA in the positive and negative NAO phases, respectively, implying a close relationship between the Atlantic-RTDW and NAO. However, because of the strengthened IL and AH, such southerly and northerly wind anomalies disappeared during the post-transition period. As a result, the relationship between the Atlantic-RTDW and NAO was weak in the latter period. In the post-transition period, an Arctic Oscillation (AO)-like pattern may resemble the Atlantic-RTDW pattern and influence Atlantic-RTDW events, which is a topic worthy of future study.

This interdecadal change has been attributed to AST activity intensity changes since the mid-1980s. Indeed, AST activity intensity experienced a decadal change from a weak regime in the pre-transition period to a strong regime in the post-transition period, as previously reported (e.g., Harnik and Chang, 2003; Lee et al., 2012). The strong AST activity intensity determined the degree of strength of the synoptic-scale eddy feedback to the mean flow. Strong feedback can induce a strong IL and AH, resulting in the disappearance of southerly wind anomalies over the NA in the post-transition period. Therefore, differing synoptic-scale feedback intensities could support wintertime NAO-related circulation anomalies over the NA in the pre- and post-transition periods, which is a potential cause for the interdecadal change in the NAO's influence on the Atlantic-RTDW-event frequency.

However, the position centers of the geopotential height tendency anomalies induced by eddy vorticity and the NAO-related circulation anomalies do not completely coincide. In addition to barotropic process, the geopotential height tendency can be induced by eddies via baroclinic processes (e.g., Lau and Holopainen, 1984; Lau and Nath, 1991). The effect of the baroclinic process on the interaction between the transient eddy and the mean flow on NAO-

related circulation anomalies will be investigated in the future.

Before 1979, direct observations in the Arctic were sparse; however, since 1979, many more satellite products were assimilated into the reanalysis data, which may have influenced interdecadal trends. The impacts of satellite products on re-analyses were investigated comprehensively by comparing re-analyses with and without assimilating satellite products (Mo et al., 1995; Kalnay et al., 1996). They concluded that the satellite data have little impact on the re-analyses in the Northern Hemisphere, implying that the data before 1979 are also relatively reliable, although direct observations in the Arctic are sparse.

Both model studies and observational results suggest that North Atlantic sea surface temperature (SST) forcing can produce NAO-like circulations (Peng et al., 2002; Han et al., 2016). Furthermore, the NAO-like circulation response to the North Atlantic SST could be elucidated by the interactions between the AST and the heating-forced anomalous flow, that is, an eddy-feedback mechanism (Peng et al., 2003), which is supported by the conclusion of our study. Meanwhile, the NAO-like circulation associated with the North Atlantic SST anomaly is disturbed by a contemporaneous sea-ice anomaly (Han et al., 2016). The winter sea ice in the North Atlantic sector of the Arctic varies significantly (Han and Li, 2018). Previous studies have concluded that it has a negative feedback effect on the NAO using model and observational data (Strong et al., 2009; Liptak and Strong, 2014). Thus, the North Atlantic SST and sea ice may affect the relationship between the NAO and Atlantic-RTDW by acting on the NAO. This possible interaction is worthy of further study.

Acknowledgements. This work was supported by National Natural Science Foundation of China (41675066) and Anhui Provincial Natural Science Foundation (1908085MD108).

Electronic supplementary material: Supplementary material is available in the online version of this article at https://doi.org/10.1007/s00376-022-2218-8.

REFERENCES

Barnston, A. G., and R. E. Livezey, 1987: Classification, seasonality and persistence of low-frequency atmospheric circulation patterns. *Mon. Wea. Rev.*, **115**, 1083–1126, https://doi.org/10.1175/1520-0493(1987)115<1083:CSAPOL>2.0.CO;2.

Blackmon, M. L., Y. H. Lee, and J. M. Wallace, 1984: Horizontal structure of 500 mb height fluctuations with long, intermediate and short time scales. *J. Atmos. Sci.*, **41**, 961–980, https://doi.org/10.1175/1520-0469(1984)041<0961:HSOMHF>2.0.CO;2.

Blackmon, M. L., J. M. Wallace, N. C. Lau, and S. L. Mullen, 1977: An observational study of the northern hemisphere wintertime circulation. *J. Atmos. Sci.*, **34**, 1040–1053, https://doi.org/10.1175/1520-0469(1977)034<1040:AOSOTN>2.0.CO;2.

Boisvert, L. N., A. A. Petty, and J. C. Stroeve, 2016: The impact of the extreme winter 2015/16 arctic cyclone on the Barents–Kara seas. *Mon. Wea. Rev.*, **144**, 4279–4287, https://doi.org/10.1175/MWR-D-16-0234.1.

Cai, M., S. Yang, H. M. Van Den Dool, and V. E. Kousky, 2007: Dynamical implications of the orientation of atmospheric eddies: A local energetics perspective. *Tellus A*, **59**, 127–140, https://doi.org/10.1111/j.1600-0870.2006.00213.x.

Chang, E. K. M., and Y. F. Fu, 2002: Interdecadal variations in Northern Hemisphere winter storm track intensity. *J. Climate*, **15**, 642–658, https://doi.org/10.1175/1520-0442(2002)015<0642:IVINHW>2.0.CO;2.

Fujibe, F., 1989: Short-term precipitation patterns in central Honshu, Japan. Classification with the fuzzy c-means method. *J. Meteor. Soc. Japan*, **67**, 967–983, https://doi.org/10.2151/jmsj1965.67.6_967.

Fujibe, F., 1999: Diurnal variation in the frequency of heavy precipitation in Japan. *J. Meteor. Soc. Japan*, **77**, 1137–1149, https://doi.org/10.2151/jmsj1965.77.6_1137.

Graham, R. M., L. Cohen, A. A. Petty, L. N. Boisvert, A. Rinke, S. R. Hudson, M. Nicolaus, and M. A. Granskog, 2017: Increasing frequency and duration of Arctic winter warming events. *Geophys. Res. Lett.*, **44**, 6974–6983, https://doi.org/10.1002/2017GL073395.

Graversen, R. G., T. Mauritsen, M. Tjernström, E. Källén, and G. Svensson, 2008: Vertical structure of recent Arctic warming. *Nature*, **451**, 53–56, https://doi.org/10.1038/nature06502.

Han, Z., and S. L. Li, 2018: Precursor role of winter sea-ice in the Labrador Sea for following-spring precipitation over southeastern North America and western Europe. *Adv. Atmos. Sci.*, **35**, 65–74, https://doi.org/10.1007/s00376-017-6291-3.

Han, Z., F. F. Luo, and J. H. Wan, 2016: The observational influence of the North Atlantic SST tripole on the early spring atmospheric circulation. *Geophys. Res. Lett.*, **43**, 2998–3003, https://doi.org/10.1002/2016GL068099.

Hanley, J., and R. Caballero, 2012: The role of large-scale atmospheric flow and Rossby wave breaking in the evolution of extreme windstorms over Europe. *Geophys. Res. Lett.*, **39**, L21708, https://doi.org/10.1029/2012GL053408.

Harnik, N., and E. K. M. Chang, 2003: Storm track variations as seen in radiosonde observations and reanalysis data. *J. Climate*, **16**, 480–495, https://doi.org/10.1175/1520-0442(2003)016<0480:STVASI>2.0.CO;2.

Hersbach, H., and Coauthors, 2020: The ERA5 global reanalysis. *Quart. J. Roy. Meteor. Soc.*, **146**, 1999–2049, https://doi.org/10.1002/qj.3803.

Honda, M., and H. Nakamura, 2001: Interannual seesaw between the Aleutian and Icelandic lows. Part II: Its significance in the interannual variability over the wintertime northern hemisphere. *J. Climate*, **14**, 4512–4529, https://doi.org/10.1175/1520-0442(2001)014<4512:ISBTAA>2.0.CO;2.

Honda, M., H. Nakamura, J. Ukita, I. Kousaka, and K. Takeuchi, 2001: Interannual seesaw between the Aleutian and Icelandic lows. Part I: Seasonal dependence and life cycle. *J. Climate*, **14**, 1029–1042, https://doi.org/10.1175/1520-0442(2001)014<1029:ISBTAA>2.0.CO;2.

Hoskins, B. J., and K. I. Hodges, 2002: New perspectives on the northern hemisphere winter storm tracks. *J. Atmos. Sci.*, **59**, 1041–1061, https://doi.org/10.1175/1520-0469(2002)059<1041:NPOTNH>2.0.CO;2.

Hoskins, B. J., I. N. James, and G. H. White, 1983: The shape, propagation and mean-flow interaction of large-scale weather systems. *J. Atmos. Sci.*, **40**, 1595–1612, https://doi.

org/10.1175/1520-0469(1983)040<1595:TSPAMF>2.0.CO;2.

Hurrell, J. W., 1995a: Decadal trends in the North Atlantic oscillation: Regional temperatures and precipitation. *Science*, **269**, 676–679, https://doi.org/10.1126/science.269.5224.676.

Hurrell, J. W., 1995b: Transient eddy forcing of the rotational flow during northern winter. *J. Atmos. Sci.*, **52**, 2286–2301, https://doi.org/10.1175/1520-0469(1995)052<2286:TEFOTR>2.0.CO;2.

Jin, F. F., 2010: Eddy-induced instability for low-frequency variability. *J. Atmos. Sci.*, **67**, 1947–1964, https://doi.org/10.1175/2009JAS3185.1.

Jin, F. F., L. L. Pan, and M. Watanabe, 2006a: Dynamics of synoptic eddy and low-frequency flow interaction. Part I: A linear closure. *J. Atmos. Sci.*, **63**, 1677–1694, https://doi.org/10.1175/JAS3715.1.

Jin, F. F., L. L. Pan, and M. Watanabe, 2006b: Dynamics of synoptic eddy and low-frequency flow interaction. Part II: A theory for low-frequency modes. *J. Atmos. Sci.*, **63**, 1695–1708, https://doi.org/10.1175/JAS3716.1.

Kalnay, E., and Coauthors, 1996: The NCEP/NCAR 40-year reanalysis project. *Bull. Amer. Meteor. Soc.*, **77**, 437–472, https://doi.org/10.1175/1520-0477(1996)077<0437:TNYRP>2.0.CO;2.

Kim, B. M., and Coauthors, 2017: Major cause of unprecedented Arctic warming in January 2016: Critical role of an Atlantic windstorm. *Scientific Reports*, **7**, 40051, https://doi.org/10.1038/srep40051.

Kug, J. S., and F. F. Jin, 2009: Left-hand rule for synoptic eddy feedback on low-frequency flow. *Geophys. Res. Lett.*, **36**, L05709, https://doi.org/10.1029/2008GL036435.

Lau, N. C., 1988: Variability of the observed midlatitude storm tracks in relation to low-frequency changes in the circulation pattern. *J. Atmos. Sci.*, **45**, 2718–2743, https://doi.org/10.1175/1520-0469(1988)045<2718:VOTOMS>2.0.CO;2.

Lau, N. C., and E. O. Holopainen, 1984: Transient eddy forcing of the time-mean flow as identified by geopotential tendencies. *J. Atmos. Sci.*, **41**, 313–328, https://doi.org/10.1175/1520-0469(1984)041<0313:TEFOTT>2.0.CO;2.

Lau, N. C., and M. J. Nath, 1991: Variability of the baroclinic and barotropic transient eddy forcing associated with monthly changes in the midlatitude storm tracks. *J. Atmos. Sci.*, **48**, 2589–2613, https://doi.org/10.1175/1520-0469(1991)048<2589:VOTBAB>2.0.CO;2.

Lee, S. S., J. Y. Lee, B. Wang, K. J. Ha, K. Y. Heo, F. F. Jin, D. M. Straus, and J. Shukla, 2012: Interdecadal changes in the storm track activity over the North Pacific and North Atlantic. *Climate Dyn.*, **39**, 313–327, https://doi.org/10.1007/s00382-011-1188-9.

Limpasuvan, V., and D. L. Hartmann, 1999: Eddies and the annular modes of climate variability. *Geophys. Res. Lett.*, **26**, 3133–3136, https://doi.org/10.1029/1999GL010478.

Limpasuvan, V., and D. L. Hartmann, 2000: Wave-maintained annular modes of climate variability. *J. Climate*, **13**, 4414–4429, https://doi.org/10.1175/1520-0442(2000)013<4414:WMAMOC>2.0.CO;2.

Liptak, J., and C. Strong, 2014: The winter atmospheric response to sea ice anomalies in the Barents Sea. *J. Climate*, **27**, 914–924, https://doi.org/10.1175/JCLI-D-13-00186.1.

Lorenz, D. J., and D. L. Hartmann, 2001: Eddy-zonal flow feedback in the Southern Hemisphere. *J. Atmos. Sci.*, **58**, 3312–3327, https://doi.org/10.1175/1520-0469(2001)058<3312:EZFFIT>2.0.CO;2.

Lorenz, D. J., and D. L. Hartmann, 2003: Eddy-zonal flow feedback in the Northern Hemisphere winter. *J. Climate*, **16**, 1212–1227, https://doi.org/10.1175/1520-0442(2003)16<1212:EFFITN>2.0.CO;2.

Luo, D. H., Y. N. Diao, and S. B. Feldstein, 2011: The variability of the Atlantic storm track and the North Atlantic oscillation: A link between intraseasonal and interannual variability. *J. Atmos. Sci.*, **68**, 577–601, https://doi.org/10.1175/2010JAS3579.1.

Magnusdottir, G., C. Deser, and R. Saravanan, 2004: The effects of North Atlantic SST and sea ice anomalies on the winter circulation in CCM3. Part I: Main features and storm track characteristics of the response. *J. Climate*, **17**, 857–876, https://doi.org/10.1175/1520-0442(2004)017<0857:TEONAS>2.0.CO;2.

Mirkin, B., 1996: *Mathematical Classification and Clustering*. Springer, 132–139, https://doi.org/10.1007/978-1-4613-0457-9.

Mo, K. C., X. L. Wang, R. Kistler, M. Kanamitsu, and E. Kalnay, 1995: Impact of satellite data on the CDAS-reanalysis system. *Mon. Wea. Rev.*, **123**, 124–139, https://doi.org/10.1175/1520-0493(1995)123<0124:IOSDAT>2.0.CO;2.

Moore, G. W. K., 2016: The December 2015 North Pole warming event and the increasing occurrence of such events. *Scientific Reports*, **6**, 39084, https://doi.org/10.1038/srep39084.

Murakami, M., 1979: Large-scale aspects of deep convective activity over the GATE area. *Mon. Wea. Rev.*, **107**, 994–1013, https://doi.org/10.1175/1520-0493(1979)107<0994:LSAODC>2.0.CO;2.

Murray, R. J., and I. Simmonds, 1995: Responses of climate and cyclones to reductions in Arctic winter sea ice. *J. Geophys. Res.: Oceans*, **100**, 4791–4806, https://doi.org/10.1029/94JC02206.

Orlanski, I., 1998: Poleward deflection of storm tracks. *J. Atmos. Sci.*, **55**, 2577–2602, https://doi.org/10.1175/1520-0469(1998)055<2577:PDOST>2.0.CO;2.

Overland, J. E., and M. Y. Wang, 2016: Recent extreme Arctic temperatures are due to a split polar vortex. *J. Climate*, **29**, 5609–5616, https://doi.org/10.1175/JCLI-D-16-0320.1.

Peng, S. L., W. A. Robinson, and S. L. Li, 2002: North Atlantic SST forcing of the NAO and relationships with intrinsic hemispheric variability. *Geophys. Res. Lett.*, **29**, 117-1–117-4, https://doi.org/10.1029/2001GL014043.

Peng, S. L., W. A. Robinson, and S. L. Li, 2003: Mechanisms for the NAO responses to the North Atlantic SST tripole. *J. Climate*, **16**, 1987–2004, https://doi.org/10.1175/1520-0442(2003)016<1987:MFTNRT>2.0.CO;2.

Pinto, J. G., T. Spangehl, U. Ulbrich, and P. Speth, 2005: Sensitivities of a cyclone detection and tracking algorithm: Individual tracks and climatology. *Meteor. Z.*, **14**, 823–838, https://doi.org/10.1127/0941-2948/2005/0068.

Rogers, J. C., 1990: Patterns of low-frequency monthly sea level pressure variability (1899-1986) and associated wave cyclone frequencies. *J. Climate*, **3**, 1364–1379, https://doi.org/10.1175/1520-0442(1990)003<1364:POLFMS>2.0.CO;2.

Screen, J. A., and I. Simmonds, 2010: The central role of diminishing sea ice in recent Arctic temperature amplification. *Nature*, **464**, 1334–1337, https://doi.org/10.1038/nature09051.

Serreze, M. C., F. Carse, R. G. Barry, and J. C. Rogers, 1997: Ice-

landic low cyclone activity: Climatological features, linkages with the NAO, and relationships with recent changes in the Northern Hemisphere circulation. *J. Climate*, **10**, 453–464, https://doi.org/10.1175/1520-0442(1997)010<0453:ILCACF>2.0.CO;2.

Strong, C., G. Magnusdottir, and H. Stern, 2009: Observed feedback between winter sea ice and the North Atlantic Oscillation. *J. Climate*, **22**, 6021–6032, https://doi.org/10.1175/2009JCLI3100.1.

Thompson, D. W. J., and J. M. Wallace, 1998: The Arctic oscillation signature in the wintertime geopotential height and temperature fields. *Geophys. Res. Lett.*, **25**, 1297–1300, https://doi.org/10.1029/98GL00950.

Thompson, D. W. J., and J. M. Wallace, 2001: Regional climate impacts of the Northern Hemisphere Annular Mode. *Science*, **293**, 85–89, https://doi.org/10.1126/science.1058958.

Trenberth, K. E., 1986: An assessment of the impact of transient eddies on the zonal flow during a blocking episode using localized Eliassen-Palm flux diagnostics. *J. Atmos. Sci.*, **43**, 2070–2087, https://doi.org/10.1175/1520-0469(1986)043<2070:AAOTIO>2.0.CO;2.

Wang, C., B. H. Ren, and J. Q. Zheng, 2019: Two impacts of arctic rapid tropospheric daily warming from different warm temperature advection on cold winters over northern hemisphere. *Earth and Space Science*, **6**, 1667–1674, https://doi.org/10.1029/2019EA000688.

Woollings, T., C. Franzke, D. L. R. Hodson, B. Dong, E. A. Barnes, C. C. Raible, and J. G. Pinto, 2015: Contrasting interannual and multidecadal NAO variability. *Climate Dyn.*, **45**, 539–556, https://doi.org/10.1007/s00382-014-2237-y.

Zhu, Q. G., J. R. Lin, S. W. Shou, and D. S. Tang, 2000: *Principles of Synoptic Meteorology*. 3rd ed. China Meteorological Press, 133–143. (in Chinese)